# Material Science

# Prof. Satish V. Kailas

Associate Professor
Dept. of Mechanical Engineering,
Indian Institute of Science,
Bangalore – 560012
India

## Chapter 8.  Failure

Failure can be defined, in general, as an event that does not accomplish its intended purpose. Failure of a material component is the loss of ability to function normally. Components of a system can fail one of many ways, for example excessive deformation, fracture, corrosion, burning-out, degradation of specific properties (thermal, electrical, or magnetic), etc. Failure of components, especially, structural members and machine elements can lead to heavy loss of lives, wealth and even may jeopardize the society! This chapter deals with the study of failures by mechanical means i.e. application stresses.

Even though the causes of failure are known, prevention of failure is difficult to guarantee. Causes for failure include: improper materials selection, improper processing, inadequate design, misuse of a component, and improper maintenance. It's the engineer's responsibility to anticipate and prepare for possible failure; and in the event of failure, to assess its cause and then take preventive measures.

Structural elements and machine elements can fail to perform their intended functions in three general ways: excessive elastic deformation, excessive plastic deformation or yielding, and fracture. Under the category of failure due to *excessive elastic deformation*, for example: too flexible machine shaft can cause rapid wear of bearing. On the other hand sudden *buckling* type of failure may occur. Failures due to excessive elastic deformation are controlled by the modulus of elasticity, not by the strength of the material. The most effective way to increase stiffness of a component is by tailoring the shape *or* dimensions. *Yielding* or *plastic deformation* may render a component useless after a certain limit. This failure is controlled by the yield strength of the material. At room temperature, continued loading over the yielding point may lead to strain hardening followed by fracture. However at elevated temperatures, failure occurs in form of time-dependent yielding known as *creep*. *Fracture* involves complete disruption of continuity of a component. It starts with initiation of a crack, followed by crack propagation. Fracture of materials may occur in three ways – brittle/ductile fracture, fatigue or progressive fracture, delayed fracture. *Ductile/brittle fracture* occurs over short period of time, and distinguishable. *Fatigue* failure is the mode in which most machine parts fail. Fatigue, which is caused by a critical localized tensile stress, occurs in parts which are

subjected to alternating or fluctuating stress. *Stress-rupture* occurs when a metal has been statically loaded at an elevated temperature for a long time, and is best example for delayed fracture.

## 8.1 Fracture, Ductile and Brittle fracture

### *8.1.1 Fracture*

Fracture is a form of failure, and is defined as the separation or fragmentation of a solid body into two or more parts under the action of stress. Fracture that occurs over a very short time period and under simple loading conditions (static i.e. constant or slowly changing) is considered here. Fracture under complex condition, for example alternating stress, is considered in later sections.

The process of fracture can be considered to be made up of two components, crack initiation followed by crack propagation. Fractures are classified *w.r.t.* several characteristics, for example, strain to fracture, crystallographic mode of fracture, appearance of fracture, etc. *Table-8.1* gives a brief summary of different fracture modes.

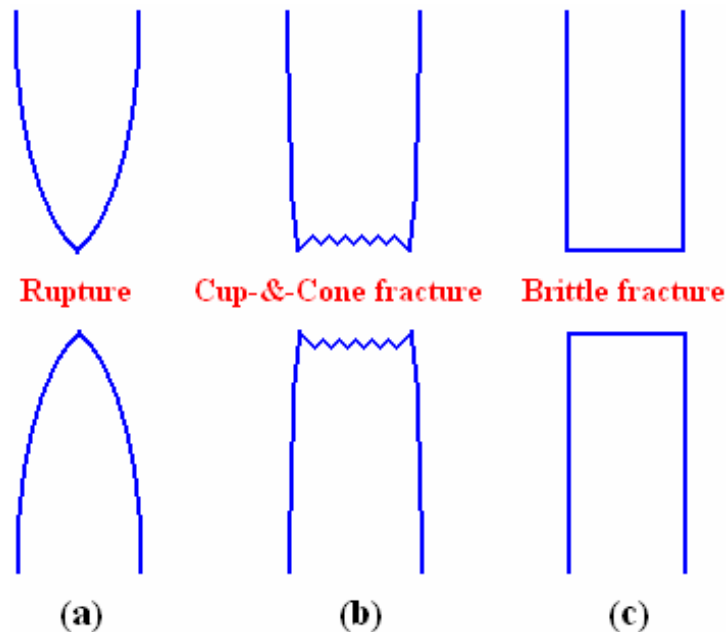**Table-8.1:** *Different fracture modes.*

| characteristic | terms used | |
|---|---|---|
| Strain to fracture | Ductile | Brittle |
| Crystallographic mode | Shear | Cleavage |
| Appearance | Fibrous and gray | Granular and bright |
| Crack propagation | Along grain boundaries | Through grains |

*Shear fracture*, promoted by shear stresses, occurs as result of extensive slip on active slip plane. On the other hand, *cleavage fracture* is controlled by tensile stresses acting normal to cleavage plane. A shear fracture surface appears gray and fibrous, while a cleavage fracture surface appears bright or granular. Actual fracture surfaces often appear as mixture of fibrous and granular mode. Based on metallographic examination of fracture surfaces of polycrystalline materials, they are classified as either transgranular or intergranular. *Transgranular fracture*, as the name go by, represents crack propagation through the grains, whereas *intergranular fracture* represents the crack that propagated along the grain boundaries.

The fracture is termed ductile or brittle depending on the ability of a material to undergo plastic deformation during the fracture. A *ductile fracture* is characterized by considerable amount of plastic deformation prior to and during the crack propagation. On the other hand, *brittle fracture* is characterized by micro-deformation or no gross deformation during the crack propagation. Plastic deformation that occurs during ductile fracture, if monitored, can be useful as warning sign to the fracture that may occur in later stages. Thus brittle fracture shall be avoided as it may occur without warning!

Since deformation of a material depends on many conditions such as stress state, rate of loading, ambient temperature, crystal structure; *ductile and brittle are relative terms*. Thus the boundary between a ductile and brittle fracture is arbitrary and depends on the situation being considered. A change from the ductile to brittle type of fracture is promoted by a decrease in temperature, an increase in the rate of loading, and the presence of complex state of stress (for example, due to a notch). Under the action of tensile stresses, most metallic materials are ductile, whereas ceramics are mostly brittle, while polymers may exhibit both types of fracture. Materials with BCC *or* HCP crystal structure can be expected to experience brittle fracture under normal conditions, whereas materials with FCC crystal structure are expected to experience ductile fracture.

*Figure-8.1* depicts characteristic macroscopic fracture profiles. The profile shown in *figure-8.1(a)* is representative of very high ductility represented by close to 100% reduction in cross-sectional area. This kind of failure is usually called *rupture*. It is observed in very soft metals such as pure gold and lead at room temperature and other metals, polymers, glasses at elevated temperatures. Most ductile metals fracture preceded by a moderate amount of necking, followed by formation of voids, cracks and finally shear. This gives characteristic *cup-and-cone fracture* as shown by *figure-8.1(b)*. In this central interior region has an irregular and fibrous appearance. *Figure-8.1(c)* presents the typical profile of brittle fracture which is usually transgranular. It occurs in most ceramics and glasses at room temperature, long-chain polymers below their glass transition temperatures, certain metals and alloys below their ductile-to-brittle transition temperatures.



**Rupture    Cup-&-Cone fracture    Brittle fracture**

(a)    (b)    (c)

**Figure-8.1:** *Fracture profiles*.

Detailed and important information on the mechanism of fracture can be obtained from microscopic examination of fracture surfaces. This study is known as *fractography*. This
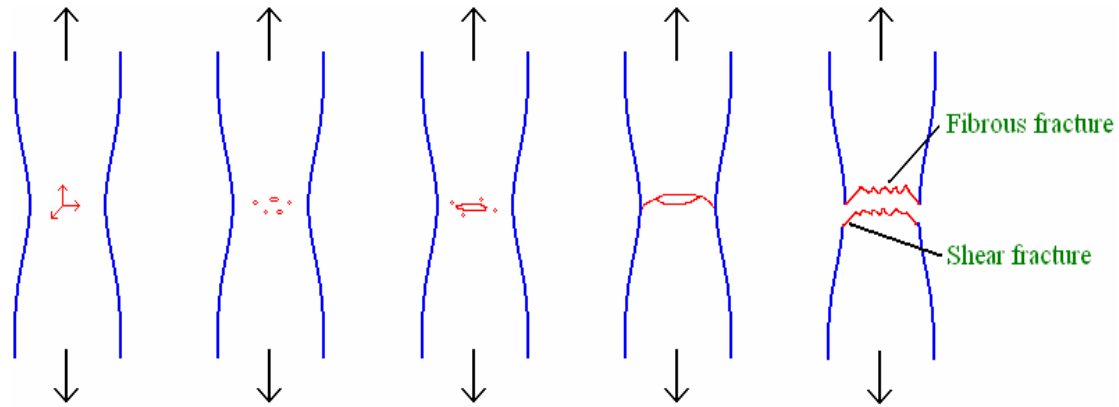
study is most commonly done using SEM (scanning electron microscope). Common microscopic modes of fracture observed include cleavage, quasi-cleavage, and dimpled rupture. Characteristic feature of cleavage fracture is flat facets, and these exhibit *river marking* caused by crack moving through the crystal along number of parallel planes which form a series of plateaus and connecting ledges. Quasi-cleavage fracture is related but distinct from cleavage in the sense that fracture surfaces are not true cleavage planes. This often exhibit dimples and tear ridges around the periphery of the facets. Dimpled rupture is characterized by cup-like depressions whose shape is dependent on stress state. The depressions may be equi-axial, parabolic, or elliptical. This dimpled rupture represents a ductile fracture. *Table-8.2* distinguishes two common modes of fracture.

**Table-8.2:** *Ductile Vs Brittle fracture.*

| *Parameter* | *Ductile fracture* | *Brittle fracture* |
|---|---|---|
| Strain energy required | Higher | Lower |
| Stress, during cracking | Increasing | Constant |
| Crack propagation | Slow | Fast |
| Warning sign | Plastic deformation | None |
| Deformation | Extensive | Little |
| Necking | Yes | No |
| Fractured surface | Rough and dull | Smooth and bright |
| Type of materials | Most metals (not too cold) | Ceramics, Glasses, Ice |

### 8.1.2 Ductile fracture

Most often ductile fracture in tension occurs after appreciable plastic deformation. It occurs by a slow tearing of the metal with the expenditure of considerable energy. It can be said that ductile fracture in tension is usually preceded by a localized reduction in cross-sectional area, called necking. Further it exhibits three stages - (1) after on set of necking, cavities form, usually at inclusions at second-phase particles, in the necked region because the geometrical changes induces hydrostatic tensile stresses, (2) the cavities grow, and further growth leads to their coalesce resulting in formation of crack that grows outward in direction perpendicular to the application of stress, (3) final failure involves rapid crack propagation at about 45 ˚to the tensile axis. This angle represents the direction of maximum shear stress that causes shear slip in the final stage. During the shear slip, crack propagates at a rapid speed around the outer perimeter of neck leaving one surface in form of cup, and the other in form of cone. Thus it is known as *cup-and-cone fracture*. In this central interior region has an irregular and fibrous appearance, which signifies plastic deformation. Different progressive stages of ductile fracture are shown in *figure-8.2*.

**Figure-8.2:** *Stages of ductile tensile fracture.*

The voids are thought to be nucleated heterogeneously at sites where further deformation is difficult. These preferred sites mainly consists of foreign inclusions, second-phase particles like oxide particles, or even voids those can form at grain boundary triple points in high-purity metals. It has been observed that concentration of nucleating sites had a strong influence on ductile fracture as true strain to fracture decreases rapidly with increasing volume fraction of second phase particles. In addition, particle shape also has an important influence. When the particles are more spherical than plate-like, cracking is more difficult and the ductility is increased. This is because dislocations can cross slip around spherical particles with ease than around plate-like particles thus avoids buildup of high stresses.

More details of fracture mechanism can be obtained from fractographic study of the fracture surface. At high magnification under microscope, numerous spherical dimples separated by thin walls are found on the ductile fractured surface. This is an indication that surface had formed from numerous holes which were separated by thin walls until it fractures. Dimples formed on shear lip of cup-and-cone fracture will be elongated attaining parabolic shape which is indication that shear failure took place.

Ductile fracture is not particularly important in terms of mechanical behavior because it usually is associated with good toughness. However, McClintock's analytical treatment of ductile fracture resulted in the following equation, which gives strain to fracture, $\varepsilon_f$,

$$\varepsilon_f = \frac{(1-n)\ln(l_0/2b_0)}{\sinh\left[(1-n)(\sigma_a + \sigma_b)/(2\overline{\sigma}/\sqrt{3})\right]}$$

for a material with a stress-strain curve given by $\sigma = K\varepsilon^n$, and $\sigma_a$, $\sigma_b$ are stresses parallel and perpendicular to the axis of the cylindrical holes respectively, $\overline{\sigma}$ is the true flow stress, $b_0$ is initial radius of cylindrical holes and $l_0$ is the average spacing of holes. The equation indicates that ductility decreases as void fraction increases, as the strain-hardening exponent, n, decreases. This is the consequence of change of stress state from uni-axial to tri-axial tension.

## 8.1.2 Brittle fracture

The other common mode of fracture is known as brittle fracture that takes place with little *or* no preceding plastic deformation. It occurs, often at unpredictable levels of stress, by rapid crack propagation. The direction of crack propagation is very nearly perpendicular to the direction of applied tensile stress. This crack propagation corresponds to successive and repeated breaking to atomic bonds along specific crystallographic planes, and hence called cleavage fracture. This fracture is also said to be transgranular because crack propagates through grains. Thus it has a grainy or faceted texture. Most brittle fractures occur in a transgranular manner. However, brittle fracture can occur in intergranular manner i.e. crack propagates along grain boundaries. This happens only if grain boundaries contain a brittle film or if the grain-boundary region has been embrittled by the segregation of detrimental elements.

In analogy to ductile fracture, as supported by number of detailed experiments, the brittle fracture in metals is believed to take place in three stages - (1) plastic deformation that causes dislocation pile-ups at obstacles, (2) micro-crack nucleation as a result of build-up of shear stresses, (3) eventual crack propagation under applied stress aided by stored elastic energy.

As mentioned earlier, brittle fracture occurs without any warning sign, thus it needs to be avoided. Hence brittle fracture and its mechanism have been analyzed to a great extent compared to ductile fracture. Brittle fracture usually occurs at stress levels well below those predicted theoretically from the inherent strength due to atomic or molecular bonds. This situation in some respects is analogous to the discrepancy between the theoretical strength shear strength of perfect crystals and their observed lower yield strength values.

When a crystal is subjected to tensile force, separation between atoms will be increased. The repulsive force decreases more rapidly with this than the attractive force, so that a net force between atoms balances the tensile force. With further increase in tensile force, repulsive force continues to decrease. At an instant, repulsive force becomes negligible because of increased separation, which corresponds to theoretical cohesive strength of the material. Assume that inter-atomic spacing of atoms in unstrained condition is $a$, and $x$ is change in mean inter-atomic distance. Strain, $\varepsilon$, is given by

$$\varepsilon = \frac{x}{a}$$

And according to Hooke's law, if $E$ – Young's modulus

$$\sigma = E\varepsilon = \frac{Ex}{a}$$

Cohesive force can be approximated with little or no error using a sine curve as follows (refer to chapter-3: theoretical strength):

$$\sigma = \sigma_{th} \sin \frac{2\pi x}{\lambda}$$

where $\lambda$ is wave length of the curve. For small values of $x$, $sin\ x \approx x$, and thus

$$\sigma = \sigma_{th} \frac{2\pi x}{\lambda}$$

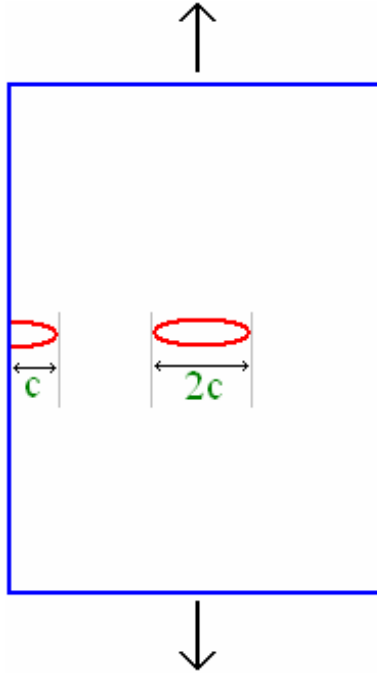If Hooke's law equation is substituted in the above equation,

$$\sigma_{th} = \frac{\lambda}{2\pi} \frac{E}{a} \approx \frac{E}{\pi}$$

In a brittle material, when fracture occurs, work expended goes into creation of two new surfaces, each with a surface energy, $\gamma$. Work done per unit area of fracture surface, $W$, is the area under the stress-strain curve.

$$W = \int_0^{\lambda/2} \sigma_{th} \sin \frac{2\pi x}{\lambda} dx = \frac{\sigma_{th}\lambda}{\pi} = 2\gamma$$

$$\Rightarrow \quad \lambda = \frac{2\pi\gamma}{\sigma_{th}} \qquad \Rightarrow \quad \sigma_{th} = \left(\frac{E\gamma}{a}\right)^{1/2}$$

As brittle fracture involves, crack propagation, let's assume that a material has an interior crack of length $2c$ (*or* a surface crack of length $c$) with radius of curvature as $\rho$ as shown in *figure-8.3*.

**Figure-8.3:** *Schematic presentation of interior and surface cracks.*

The maximum stress at the tip of crack is

$$\sigma_{max} = \sigma\left[1 + 2\left(\frac{c}{\rho}\right)^{1/2}\right] \approx 2\sigma\left(\frac{c}{\rho}\right)^{1/2}$$

Before fracture starts, maximum stress at the crack tip shall rise to theoretical value of cohesive strength. Once both are equal, crack propagates. The stress is then can be called *nominal fracture stress*, $\sigma_f$, is given by

$$\sigma_f \approx \left(\frac{E\gamma\rho}{4ac}\right)^{1/2}$$

The sharpest crack (i.e. maximum stress concentration) can be represented by $\rho = a$. Thus,

$$\sigma_f \approx \left(\frac{E\gamma}{4c}\right)^{1/2}$$

<u>Griffith theory</u>: Griffith proposed that a brittle material contains number of micro-cracks which causes stress rise in localized regions at a nominal stress which is well below the theoretical value. When one of the cracks spreads into a brittle fracture, it produces an increase in the surface energy of the sides of the crack. Source of the increased surface energy is the elastic strain energy, released as crack spreads. *Griffith's criteria* for

propagation of crack include these terms as: <u>a crack will propagate when the decrease in elastic energy is at least equal to the energy required to create the new crack surface</u>. This criterion is useful in determining the tensile stress which will just cause a critical sized crack to propagate as a brittle fracture.

Elastic energy stored under tensile stress will be released as crack propagates. Part of this energy is expended in forming the surface of the crack, while the remaining is transformed into kinetic energy. According to Griffith, such as crack will propagate and produce brittle fracture when an incremental increase in its length doe not change the net energy of the system. Strain energy released in a thin plate of unit thickness is given by Inglis as follows:

$$U_e = \frac{\pi \sigma^2 c^2}{E}$$

where $E$ is Young's modulus, and is the applied stress. At the same time, surface energy gained by the system due to new surfaces formed as a crack, of length $2c$, propagates can be given as

$$U_s = 4\gamma c$$

Griffith's criterion can be expressed as follows for incremental change in systems energy with crack length:

$$\frac{\partial U_e}{\partial c} = \frac{\partial U_s}{\partial c} \quad \Rightarrow \quad \frac{2\pi \sigma^2 c}{E} = 4\gamma \quad \Rightarrow \quad \sigma = \left(\frac{2E\gamma}{c\pi}\right)^{1/2}$$

The equation gives the stress required to propagate a crack in a thin plate under plane stress. The stress necessary to cause fracture varies inversely with length of existing cracks, thus largest crack determines the strength of material. The sensitivity of the fracture of solids to surface conditions has been termed *Joffe effect*. For a plate which is thick compared with crack size (i.e. plane strain condition), the stress is given as

$$\sigma = \left(\frac{2E\gamma}{(1-v^2)c\pi}\right)^{1/2}$$

where $v$ is Poisson's ratio. The Griffith theory applies only to completely brittle materials. In crystalline materials which fracture in an apparently brittle mode, plastic deformation usually occurs next to fracture surface. Orowan, thus, modified the Griffith equation to make it more compatible by including plastic energy term as follows:

$$\sigma = \left(\frac{2E(\gamma + p)}{c\pi}\right)^{1/2} \approx \left(\frac{Ep}{c}\right)^{1/2}$$

where p is the work of plastic deformation at the tip of the growing crack. The surface energy term is neglected in the above equation since plastic work values are in order of $10^2$-$10^3$ J m$^{-2}$ as compared to surface energy values whose range is 1-2 J m$^{-2}$.

## 8.2 Fracture mechanics

It is a relatively new section of materials study under mechanical loading conditions. Using fracture mechanics concept it possible to determine whether a crack of given length in a material with known toughness is dangerous at a given stress level. This mechanics section can also provides guide lines for selection of materials and design against fracture failures.

Orowan modified equation is further modified by Irwin to replace the hard to measure plastic work term with other term that was directly measurable. New form of the equation

$$\sigma = \left( \frac{EG_c}{c\pi} \right)^{1/2}$$

where $G_c$ is the critical value of *crack-extension force*.

$$\Rightarrow \quad G = \frac{\pi\sigma^2 c}{E}$$

$G$ has units of J m$^{-2}$, and is actually *strain-energy release rate* that is experimentally measurable. The critical value of crack extension force, $G_c$, makes the crack propagate to fracture, and is considered as one form of *fracture toughness* of the material. Fracture toughness is defined as fracture resistance of a material in the presence of cracks.

Fracture occurs due to *stress concentration* at flaws, like surface scratches, voids, etc. If **c** is the length of the crack and $\rho$ the radius of curvature at crack tip, the enhanced stress ($\sigma_m$) near the crack tip is given by:

$$\sigma_m = 2\sigma \left( \frac{c}{\rho} \right)^{1/2}$$

The above equation states that smaller the radius, higher is the stress enhancement. Another parameter, often used to describe fracture toughness is known as critical *stress concentration factor*, *K*, and is defined as follows for an infinitely wide plate subjected to tensile stress perpendicular to crack faces:

$$K = \sigma\sqrt{c\pi}$$

This relation holds for specific conditions, and here it is assumed that the plate is of infinite width having a through-thickness crack. It is worth noting that *K* has the unusual
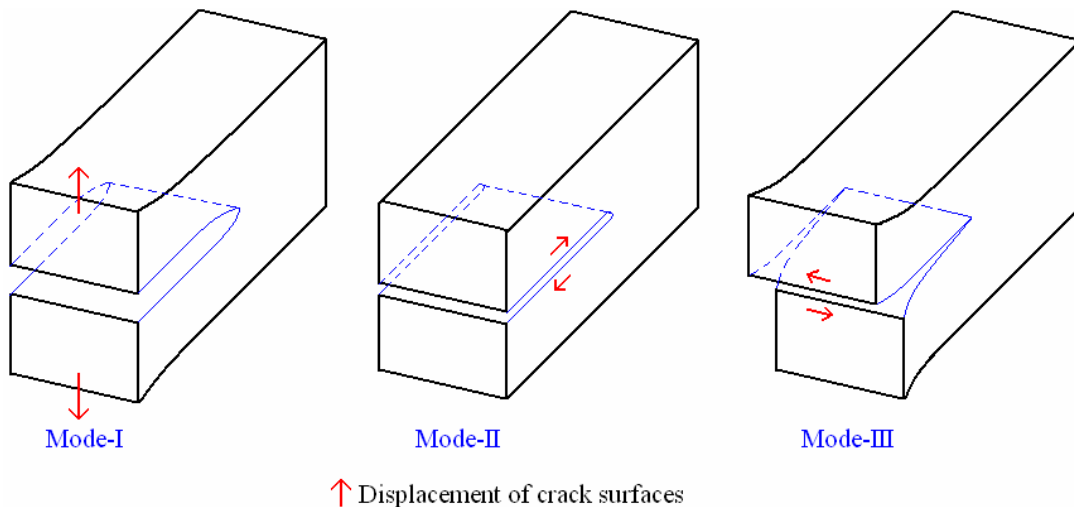
units of MPa√m. It is a material property in the same sense that yield strength is a material property. The stress intensity factor $K$ is a convenient way of describing the stress distribution around a flaw. For the general case the stress intensity factor is given by

$$K = \alpha \sigma \sqrt{c\pi}$$

where $\alpha$ is a parameter that depends on the specimen and crack sizes and geometries, as well as the manner of load application. For example, for a plate of width $w$ loaded in tension with a centrally located crack of length $2c$,

$$K = \alpha \sigma \sqrt{c\pi} = \sigma \sqrt{c\pi} \left( \frac{w}{c\pi} \tan \frac{c\pi}{w} \right)^{1/2}$$

In this regard, it is important to realize that there are three basic modes of fracture, as shown in *figure-8.4*. *Mode-I* corresponds to fracture where the crack surfaces are displaced normal to themselves. This is a typical tensile type of fracture. In *mode-II*, crack surfaces are sheared relative to each other in a direction normal to the edge of the crack. In *mode-III*, shearing action is parallel to the edge of the crack. To indicate different modes, it is normal practice to add the corresponding subscript. The above example described is obviously of the mode-I. There are two extreme cases for mode-I loading. With thin plate-type specimens the stress state is plane stress, while with thick specimens there is a plane-strain condition. The plane-strain condition represents the more severe stress state and the values of $K$ are lower than for plane-stress specimens. The fracture toughness measured under plane-strain conditions is obtained under maximum constraint or material brittleness. The plane strain fracture toughness is designated as $K_{Ic}$, and is a true material property.



↑ Displacement of crack surfaces

**Figure-8.4:** *Crack deformation modes*.

While crack extension force, $G$, has more direct physical significance to the fracture process, the stress intensity factor $K$ is preferred in working with fracture mechanics because it is more amenable to analytical determination. Both these parameters are related as:

$$K^2 = GE \qquad \text{for plane stress (e.g. thin plate)}$$

$$K^2 = GE/(1-v^2) \qquad \text{for plane strain (e.g. thick plate)}$$

Fracture toughness for mode-I, plane strain fracture toughness $K_{Ic}$, depends on many factors, the most influential of which are temperature, strain rate, and microstructure. The value of $K_{Ic}$ decreases with increasing strain rate and decreasing temperature. Normally values of $K_{Ic}$ increases with reduction in grain size. In addition, an enhancement in yield strength generally produces a corresponding decrease in $K_{Ic}$. The minimum thickness to achieve plane-strain conditions and valid $K_{Ic}$ measurements is

$$B = 2.5\left(\frac{K_{Ic}}{\sigma_0}\right)^2$$

where $\sigma_0$ is the 0.2% offset yield strength.

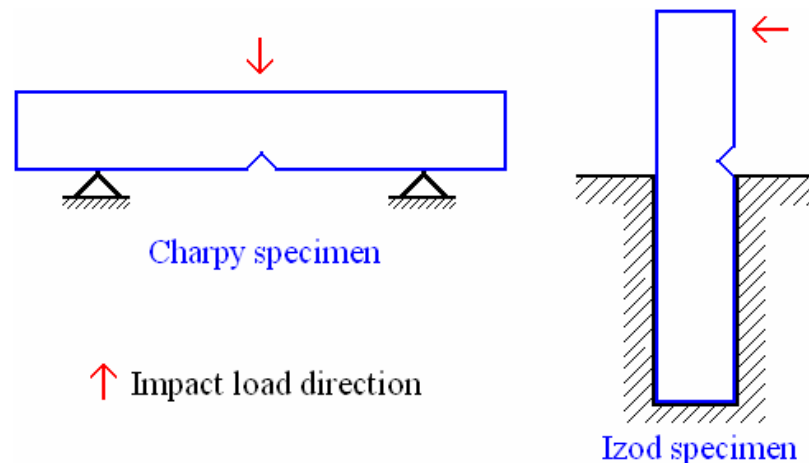## 8.3 Impact fracture testing, Ductile-to-Brittle transition

### 8.3.1 Impact fracture testing

As mentioned in earlier section, three basic factors contribute to a brittle-cleavage type of fracture. They are (1) tri-axial state of stress (2) a low temperature and (3) a high strain rate or rapid rate of loading. A tri-axial state of stress, such as exists at a notch, and low temperature are responsible for most service failures of brittle type. Since, these effects are accented at a high rate of loading, various types of notched-bar impact tests have been used to determine the susceptibility of materials to brittle fracture.

The changes produced by the introduction of a notch have important consequences in the fracture process. The chief effect of the notch is not in introducing a stress concentration but in producing a tri-axial state of stress at the notch. As a result of this tri-axial state of stress, yield strength of a notched specimen is greater than the uni-axial yield strength because it is more difficult to spread the yielded zone in the presence of tri-axial stresses. The ratio of notched-to-unnotched strength is referred as the *plastic-constraint factor*, *q*. Unlike stress concentration factor, which can reach values in excess of 10 as the notch is made sharper and deeper, Orowan has shown that the plastic constraint factor cannot exceed a value of 2.57. It results in notch-strengthening of a ductile material. But in a material prone to brittle fracture the increased tensile stresses from the plastic constraint can exceed the critical value for fracture before the material undergoes general plastic yielding. A notch, thus, increases the tendency for brittle fracture in four important ways: (a) By producing high local stresses, (b) by introducing a tri-axial state of stress, (c) by

producing high local strain hardening and cracking, and (d) by producing a local magnification to the strain rate.

Two classes of specimens have been standardized for notch-impact testing: (i) Charpy specimen. It has a square cross section and contains 45 ˚ V notch, 2 mm deep with a 0.25 mm root radius. The specimen is supported as a horizontal beam, and loaded behind the notch by the impact of heavy swinging pendulum with velocity about 5 m/sec. The energy expended is measured in terms of change in potential energy (height) of the pendulum. The specimen is forced to bend and fracture at a high strain rate in order of $10^3$ sec$^{-1}$. The V-notch in the specimen provides triaxiality of stress, and the high hammer velocity insures a high strain rate. (ii) Izod specimen. It has either circular *or* square cross section and contains V notch near the clamped end. It is supported as over hanging vertical beam. Load is again applied using swinging pendulum but in front of the notch. *Figure-8.5* depicts loading of Charpy and Izod specimens for notch-impact tests.



**Figure-8.5:** *Loading of Charpy and Izod notched-bar impact testing specimens*.
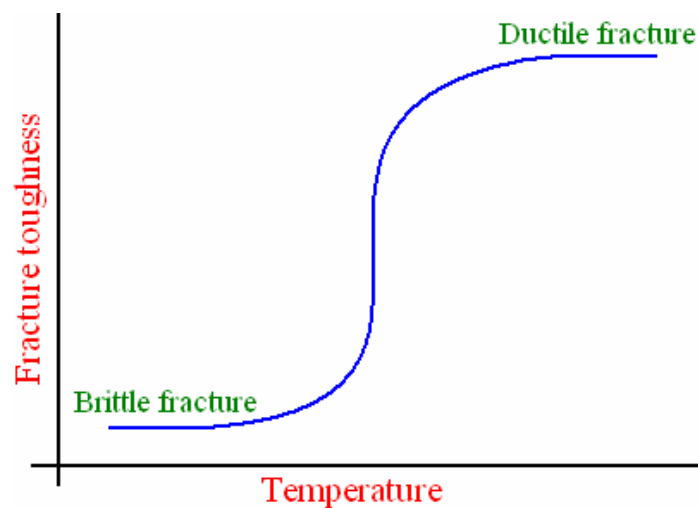
The principal measurement from the impact test is the energy absorbed in fracturing the specimen. Energy expended during fracture is some times known as *notch toughness*. The energy expended will be high for complete ductile fracture, while it is less for brittle fracture. However, it is important to note that measurement of energy expended is only a relative energy, and can not be used directly as design consideration. Another common result from the Charpy test is by examining the fracture surface. It is useful in determining whether the fracture is fibrous (shear fracture), granular (cleavage fracture), or a mixture of both. A third measurement that can be made is the ductility, indicated by the percent contraction of the specimen at the notch. The notched-bar impact test is most useful when conducted over a range of temperatures. Thus it is possible to know at which temperature the ductile-to-brittle transition is taking place. Thus the chief engineering use of Charpy test is in selecting materials which are resistant to brittle fracture by means of transition temperature curves. When selecting a material for design purposes which might be susceptible to brittle fracture, the material with the lowest transition temperature is to be preferred.

Both plane strain fracture toughness and notched-bar impact tests determine the fracture properties of materials. The former are quantitative in nature, in that a specific property is determined. On the other hand, the results of the impact tests are qualitative in nature, thus are of little use fro design purposes. Plane strain fracture toughness tests are not as simple to perform as impact tests, and equipment and specimens are more expensive.

### 8.3.2 Ductile-to-Brittle transition

It is well understood that ductile and brittle are relative, and thus interchange between these two modes of fracture is achievable with ease. The term *Ductile-to-Brittle transition* (DBT) is used in relation to the temperature dependence of the measured impact energy absorption. For a material, as the temperature is lowered, the impact energy drops suddenly over a relatively narrow temperature range, below which the energy has a considerably lower value as a representative of brittle fracture.

The temperature where DBT occurs is termed as *Ductile-to-Brittle Transition Temperature* (DBTT). A typical variation of energy expended as a function of temperature is shown in *figure-8.6*. From the figure it can be concluded that there is no single criterion that defines the transition temperature. Above the DBTT, the yield strength ($\sigma_y$) is lower than the tensile stress necessary to cause brittle failure ($\sigma_f$) i.e. $\sigma_y < \sigma_f$. With decreasing temperature, the yield strength increases rapidly to the point where it equals the tensile stress for brittle failure, and below this temperature, fracture usually occurs in brittle/cleavage mode. So, at and below the DBTT, $\sigma_y = \sigma_f$. At the transition temperature, the micro-cracks that form are of critical size for crack propagation, and at lower temperatures these cracks exceed the critical size. Over a temperature range just above DBTT, micro-cracks formed are initially sub-critical so that further plastic deformation and strain hardening must proceed before the tensile stress level becomes sufficient to cause crack propagation. With further increase in temperature, micro-cracks no longer form and fracture mode changes from cleavage to ductile.



**Figure-8.6:** *Typical variation of fracture toughness as a function of temperature.*

As shown in the above figure, BCC metals possess a distinct DBTT compared with other metals. Common BCC metals are to become brittle at low temperatures or at extremely high rates of strain. Many FCC metals, on the other hand, remain ductile even at very low temperatures. In metals DBTT is around 0.1-0.2 $T_m$ while in ceramics it is about 0.5-0.7 $T_m$, where $T_m$ represents absolute melting temperature. The crack propagation stress usually is relatively insensitive to temperature. Strain rate which increases the yield strength but not the crack propagation stress increases the DBTT. As mentioned earlier, DBTT does not have a unique value for a given material, and is a function of several other variables such as flaw size, strain rate, triaxiality of stress, etc. Sharp notches in the specimen provide stress concentration centers and thus increase the DBTT. Fine grained materials have a lower transition temperature as compared to coarse grained materials.

There are other factors which affect the DBTT for a material, for example metallurgical factors. One of the most important is microstructure, which in turn can depend on heat treatment practice and temperature, for example, for steels. The composition also has a very pronounced effect on DBTT. In steels, it is found that impurities like P, Si, Mo, Cr along with C increase the DBTT, while Mn and Ni have reverse effect.
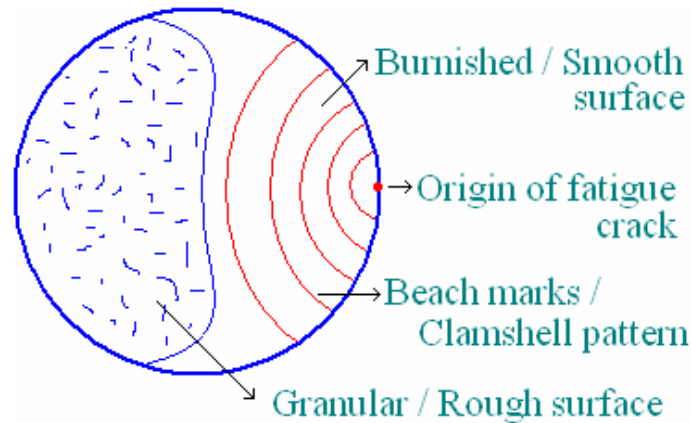
## 8.4 Fatigue, Crack initiation and propagation, Crack propagation rate

### 8.4.1 Fatigue

Failures occurring under conditions of dynamic or alternating loading are called *fatigue failures*, presumably because it is generally observed that these failures occur only after a considerable period of service. Fatigue failure usually occurs at stresses well below those required for yielding, or in some cases above the yield strength but below the tensile strength of the material. These failures are dangerous because they occur without any warning. Typical machine components subjected to fatigue are automobile crank-shaft, bridges, aircraft landing gear, etc. Fatigue failures occur in both metallic and non-metallic materials, and are responsible for a large number fraction of identifiable service failures of metals.

A typical fatigue-fracture surface looks like the one shown in *figure-8.7*. The fatigue crack nucleates at the stress concentration. Generally, the fatigue fracture surface is perpendicular to the direction of an applied stress. A fatigue failure can be recognized from the appearance of the fracture surface, which shows a smooth and polished surface that corresponds to the slow growth of crack, when the crack faces smoothen out by constant rubbing against each other and a rough/granular region corresponds to the stage of fast growth, after critical conditions is attained where member has failed in a ductile manner when cross section was no longer able to carry the applied load. The region of a fracture surface that formed during the crack propagation step may be results in characteristic pattern of concentric rings spread over the smooth region of the fracture surface, known as *beach marks or* striations, radiating outward from the point of initiation of the failure, as shown in *figure-8.7*. Beach marks (also known as *clamshell pattern*) are macroscopic dimensions and may be observed with the unaided eye. These markings are found for components that experienced interruptions during the crack

propagation stage.  Each beach mark band represents a period of time over which crack growth occurred. On the other hand fatigue striations are microscopic in size and subject to observation with the electron microscope (either TEM or SEM). The relatively widely spaced striations are caused by variations in the stress amplitude during the life of the component. On a much finer level, a large number of striations may be sometimes being seen. The width of each striation here is equal to the distance by which the crack grows during one cycle.  Any point with stress concentration such as sharp corner *or* notch *or* metallurgical inclusion can act as point of initiation of fatigue crack.



**Figure-8.7:** *Schematic of fatigue fracture surface.*

Three basic requisites for occurrence of fatigue fracture are: (a) a maximum tensile stress of sufficiently high value (b) a large enough variation or fluctuation in the applied stress and (c) a sufficiently large number of cycles of applied stress. The stress cycles that are evident in fatigue studies are characterized using many parameters, such as mean stress, alternating stress, stress ratio and amplitude ratio. If the applied stress varies between $\sigma_{max}$ and $\sigma_{min}$,

Range of stress, $\sigma_r = \sigma_{max} - \sigma_{min}$

Alternating stress, $\sigma_a = \sigma_r/2 = (\sigma_{max} - \sigma_{min})/2$

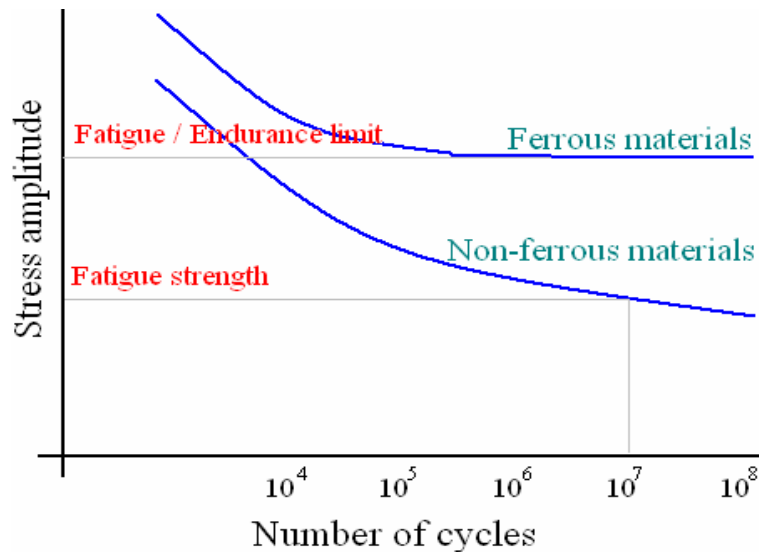Mean stress, $\sigma_m = (\sigma_{max} + \sigma_{min})/2$

Stress ratio, $R = \sigma_{min} / \sigma_{max}$

Amplitude ratio, $A = \sigma_a / \sigma_m = (1-R) / (1+R)$

There are as many ways of conducting a test to measure fatigue as there are ways of applying repeated stresses to a metal. A specimen of rotating beam type is often used because of its simplicity. In a fatigue test, the premium output is number of cycles required to fracture the specimen at a given stress. If the maximum tensile stress applied

is only slightly less than the yield strength (*or* tensile strength), test will run only a few cycles. Continues reduction of the stress greatly increases the life of the specimen, hence fatigue data is usually presented by plotting maximum stress (*S*) against number of cycles to fracture (*N*), using a logarithmic scale for the latter variable. This form of curve, *S-N* curve, shown in *figurer-8.8*, is significant because there is a stress below which the specimens do not fracture. This limiting stress is called *fatigue limit* or *endurance limit* ($\sigma_e$), below which fatigue will never occur. Fatigue limit can be related to tensile strength of the material, and the ratio of fatigue limit to tensile strength is known as *endurance ratio*. Most steels have distinct fatigue limit, and is usually about 0.4-0.5 of tensile strength i.e. endurance ratio=0.4-0.5. Unlike steels, most nonferrous metals do not have a fatigue limit i.e. *S-N* curve continues to fall steadily with decreasing stress, though at a decreasing rate. Thus, fatigue will ultimately occur regardless of the magnitude of the applied stress. Fatigue response of these materials is specified for a number of stress cycles, normally $10^7$, and is known as *fatigue strength*. Another important parameter that characterizes a material's fatigue behavior is *fatigue life*, $N_f$, number of cycles to cause fatigue failure at a specified stress level.
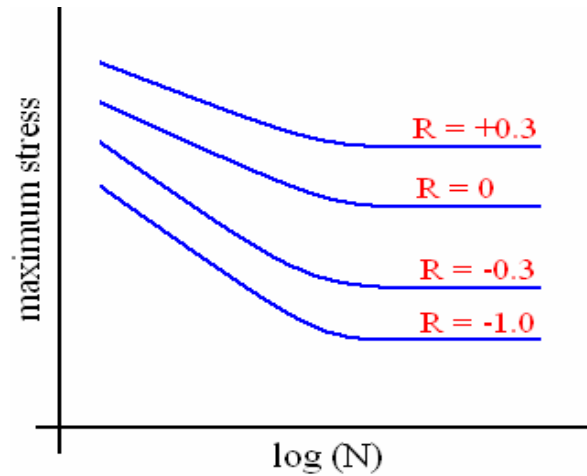


**Figure-8.8:** *Typical S-N curves for ferrous and non-ferrous metals*.

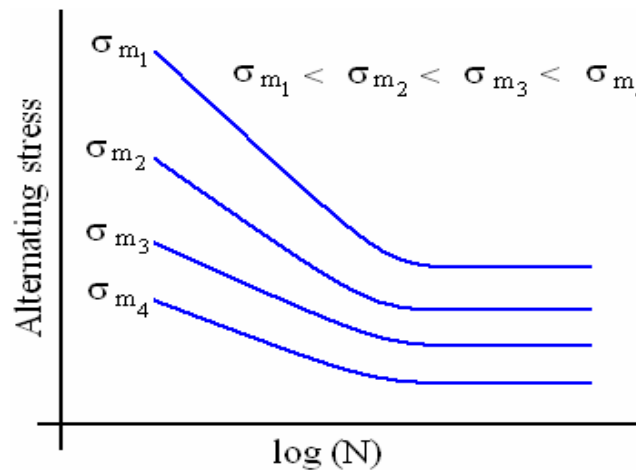The S-N curve in the high-cycle region is some times described by the Basquin equation:

$$N\sigma_a^p = C$$

where $\sigma_a$ is the alternating stress or stress amplitude and *p* and *C* are empirical constants. It will be generally found that there is a considerable amount of scatter in the results. Thus fatigue life and fatigue strength are considered as statistical quantities. It has been observed that scatter in fatigue life decreases with increase in stress. The statistical problem of accurately determining the fatigue limit is complicated by the fact that complete S-N curve cannot obtainable using a single specimen as specimen cannot be rested during the test.

With the exception of rotating shafts, most structural members are not subjected to symmetrical stress cycles having a mean stress of zero. When ($R$ = -1 for the case of completely reversed stress) $R$ becomes more positive i.e. with increasing mean stress, the measured fatigue limit becomes greater (*figure-8.9*). For a given stress amplitude, a mean tensile stress reduces the fatigue life of a material. It has been observed that as the mean stress becomes more positive the allowable alternating stress decreases (*figure-8.10*).
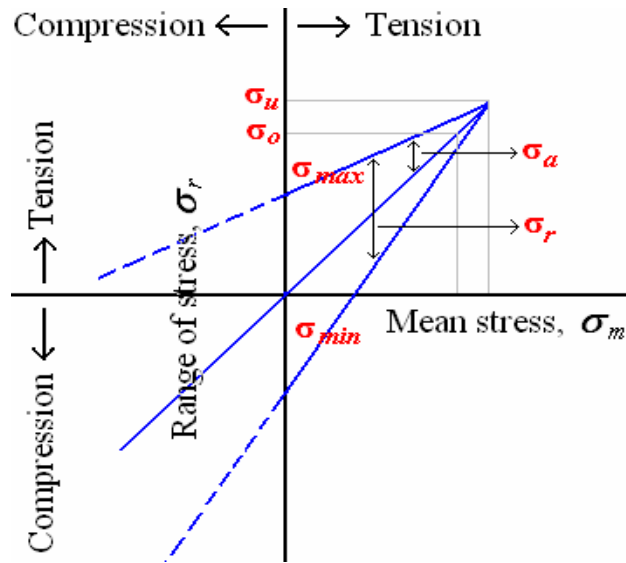


**Figure-8.9:** *Dependence of fatigue limit on stress ratio.*



**Figure-8.10:** *Dependence of alternating stress on mean stress.*

The Goodman diagram presents the dependence of allowable stress ranges on mean stress for a material. As shown in *figure-8.11*, allowable stress range increases with increasing compressive mean stress i.e. compressive stress increases the fatigue limit.
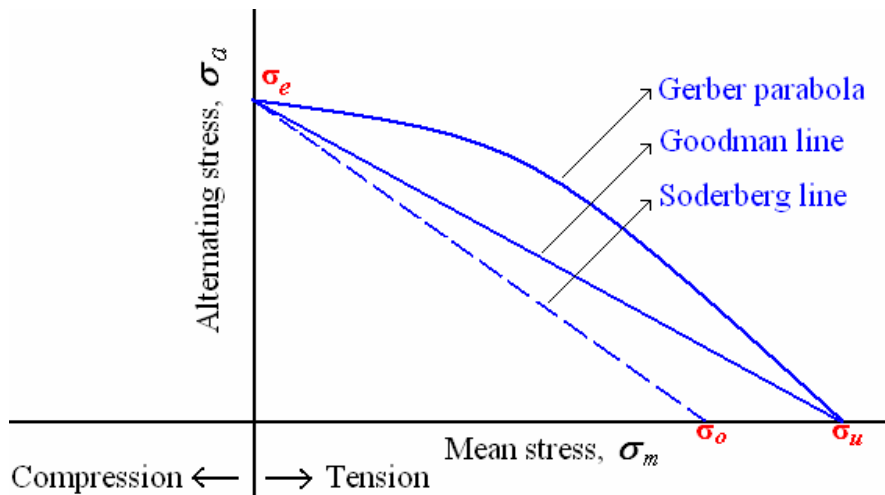
**Figure-8.11:** *Goodman diagram.*

An alternative method of presenting mean stress data is by using Heig-Soderberg diagram in which alternating stress is plotted against the mean stress. As *figure-8.12* depicts, Goodman's criterion appears as a straight line. Test data for ductile metals, however, follows parabolic curve proposed by Gerber. Both these criteria can be expressed as:

$$\sigma_a = \sigma_e \left[ 1 - \left( \frac{\sigma_m}{\sigma_u} \right)^x \right]$$

where $x=1$ for Goodman line, $x=2$ for the Gerber parabola, and $\sigma_e$ is the fatigue limit for completely reversed loading. Soderberg line presents the data when the design is based on yield strength ($\sigma_0$).



**Figure-8.12:** *Heig-Soderberg diagram.*
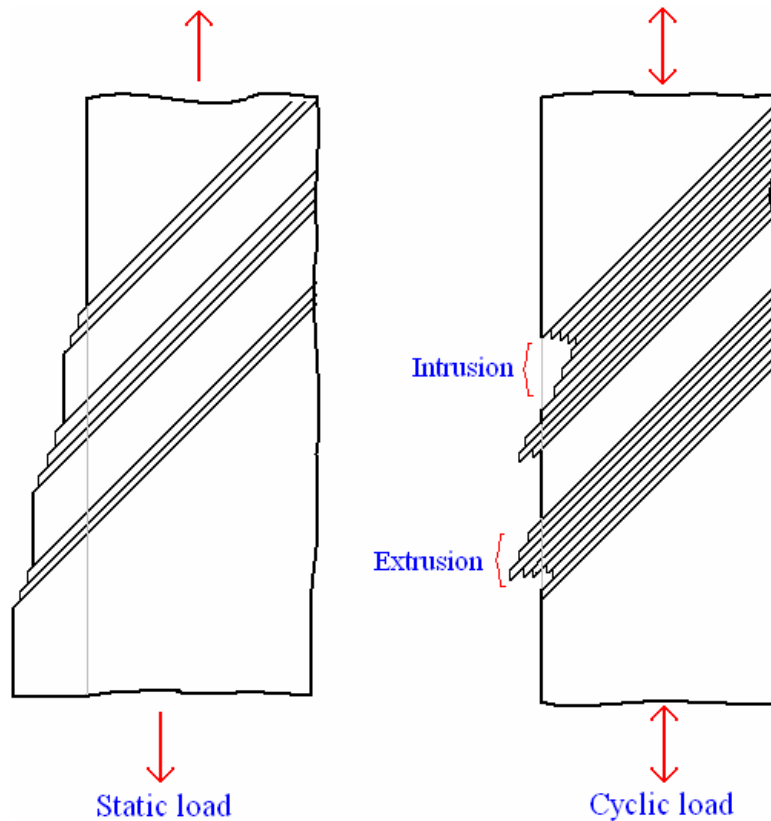
### 8.4.2 Crack initiation and propagation

Based on structural changes that occur during fatigue, fatigue failure process can be considered as made of following stages: (a) crack initiation – includes the early development of fatigue damage that can be removed by suitable thermal anneal (b) slip-band crack growth – involves the deepening of initial crack on planes of high shear stress. This is also known as stage-I crack growth. (c) crack growth on planes of high tensile stress – involves growth of crack in direction normal to maximum tensile stress, called stage-II crack growth (d) final ductile failure – occurs when the crack reaches a size so that the remaining cross-section cannot support the applied load.

Fatigue failures usually are found to initiate at a free surface or at internal flaws such as inclusions where the local stress causes some heterogeneous permanent flow leading to formation of a small crack. Fatigue failures start as small microscopic cracks and, accordingly, are very sensitive to even minute stress raisers. It has been observed that diffusion processes are not necessary to the formation of fatigue cracks. The initiation of a fatigue crack does not lead to immediate failure, rather, the crack propagates slowly and discontinuously across the specimen under the action of cyclic stress. The amount of crack motion per cycle depends on the material and the stress level; high stresses favor larger crack growth increments per cycle. Eventually, the crack propagates to the point where the remaining intact cross section of material no longer can support the applied load, and further crack propagation is rapid, leading to catastrophic failure. The final fracture surface is composed of an area over which there was slow crack propagation and an area where the crack moved rapidly. Final fracture can be either ductile or brittle type.

In polycrystalline metals, during a fatigue test slip lines appear first on crystal whose slip planes have the highest resolved shear stress. As time goes on and the number of stress cycles increases, the size and number of slip bands (clusters of slip lines) increase. The extent and number of slip bands are also a function of the amplitude of the applied stress; higher stresses give larger values. In fatigue, under cyclic loading, the slip bands tend to group into packets or striations in a slip band. Each striation represents the successive position of an advancing crack front that is normal to the greatest tensile stress. Ridge kinds of striations are called *extrusions* while, while crevice striations are known as *intrusions*, and both tend to be formed depending on the crystal orientation. It has been shown that fatigue cracks initiate at intrusions and extrusions. These surface disturbances are approximately $10^{-3}$ to $10^{-4}$ mm in height and appear as early as 1/10 of the total life of a specimen. *Figure-8.13* depicts the slip bands forming under static load and cyclic load. *Table-8.3* summarizes deformation features under static and cyclic loading.

With increasing numbers of cycles, the surface grooves deepen and the crevices *or* intrusions take on the nature of a crack. When this happens, stage-I of the crack-growth process has begun i.e. stage-I crack propagates along persistent slip bands, and can continue for a large fraction of the fatigue life. Low applied stresses and deformation by slip on a single slip plane favor stage-I growth. On the other hand multiple-slip conditions favor stage-II growth. The transition from stage-I to stage-II is often induced when a slip-plane crack meets an obstacle such as a grain boundary. The rate of crack

propagation in stage-I is generally very low on the order of nm per cycle compared with that in stage-II where it is in order of μm per cycle. Thus, from a practical viewpoint, stage-II is of importance than stage-I. Stage-I growth follows a slip plane, whereas stage-II growth does not have this crystallographic character. The fracture surface of stage-I is practically featureless. On the other hand, stage-II shows a characteristic pattern of striations, which occurs by repetitive plastic blunting and sharpening of the crack tip. *Table-8.4* distinguishes stage-I from stage-II crack growth.



**Figure-8.13:** *Comparison of slip bands formed under (a) static loading and (b) cyclic loading.*

**Table-8.3:** *Deformation under static and cyclic loads.*

| Feature | Static load | Cyclic load |
|---|---|---|
| Slip (*nm*) | 1000 | 1-10 |
| Deformation feature | Contour | Extrusions & Intrusions |
| Grains involved | All grains | Some grains |
| Vacancy concentration | Less | Very high |
| Necessity of diffusion | Required | Not necessary |

**Table-8.4:** *Fatigue crack growth: stage-I Vs stage-II.*

|  | *Stage-I* | *Stage-II* |
|---|---|---|
| Stresses involved | Shear | Tensile |
| Crystallographic orientation | Yes | No |
| Crack propagation rate | Low (nm/cycle) | High (µm/cycle) |
| Slip on | Single slip plane | Multiple slip planes |
| Feature | Feature less | Striations |

The region of fatigue fracture surface that formed during the crack propagation step can be characterized by two types of markings termed *beach marks* and *striations*. Both of these features indicate the position of the crack tip at some point in time and appear as concentric rings that expand away from the crack initiation site(s), frequently in a circular or semicircular pattern. Beach marks (some times also called *clamshell marks*) are of macroscopic dimensions, found for components that experienced interruptions during the crack propagation stage. Each beach mark band represents a period of time over which crack growth occurred. Striations are microscopic in size, and each of it is thought to represent the advance distance of a crack front during a single load cycle. Striation width depends on, and increases with, increasing stress range. There may be literally thousands of striations within a single beach mark. The presence of beach marks/striations on a fracture surface confirms that the cause of failure in fatigue. Nevertheless, the absence of either or both does not exclude fatigue as the case of failure.

### 8.4.3 Crack propagation rate

As pointed out in earlier section, crack propagation in stage-II, where it is faster, has greater practical importance. Considerable research has gone into studying the crack propagation in this stage as the results from this can be used as fail-safe design considerations.

To distinguish the crack propagation time from crack initiation time, pre-existing flaws or cracks are introduced into a fatigue specimen. Crack propagation rate (*da/dN*) is studied in terms of increase in crack growth which is a proportional to number of applied stress cycles and length of the crack i.e.

$$\frac{da}{dN} = fn(\sigma, a) = C\sigma_a^m a^n$$

where C – a constant, $\sigma_a$ – the alternating stress, *a* – the crack length, *m*=2-4, and *n*=1-2.

It has been found that crack growth rate can be related to stress-intensity factor, *K* (mode-I) of fracture mechanics which itself is a combination of stress and crack length. Thus,

$$\frac{da}{dN} = A(\Delta K)^p$$

where $\Delta K$ – stress-intensity factor range., $A$ and $p$ – constants that are functions of material, environment, frequency, temperature and stress ratio.

$$\Delta K = K_{max} - K_{min} = \sigma_{max}\sqrt{a\pi} - \sigma_{min}\sqrt{a\pi} = \sigma_r\sqrt{a\pi}$$

Since the stress intensity factor is not defined for compressive stresses, if $\sigma_{min}$ is in compression, zero value is assigned for $K_{min}$.
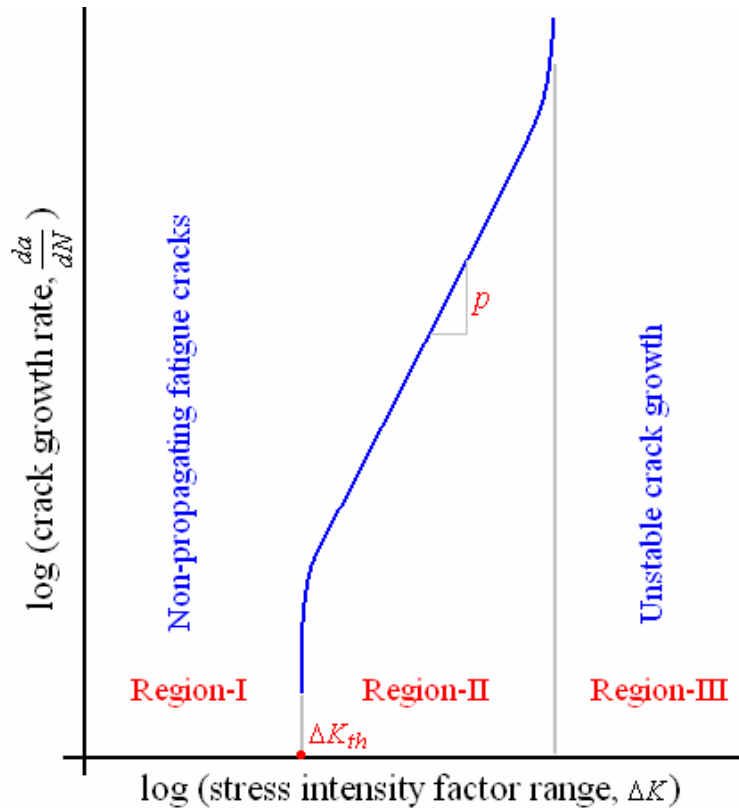
Fatigue data presented in terms of log (crack growth rate) against log ($\Delta K$) is shown in *figure-8.14*. The curve can be divided into three regions. In region-I, which is bound by a threshold value $\Delta K_{th}$, no observable crack growth occurs i.e. crack growth rate is very slow in order of 0.25 nm per cycle or less. The straight line part of curve in region-II can be represented by the power law (also known as *Paris law*)

$$\frac{da}{dN} = A(\Delta K)^p$$

and slope of the straight line will give value for $p$. The values of p are the range of 3 for steels, and in the range of 3-4 for aluminium alloys. Region-III of the curve represents the rapid unstable crack growth to ultimate fracture. Here $K_{max}$ approaches $K_c$, the fracture toughness of the material. When $K$ is known under relevant loading conditions, the fatigue life can be estimated by integrating the above equation between limits of initial crack size and final crack size. One such equation is given below when $p \neq 2$:

$$N_f = \frac{a_f^{-(m/2)+1} - a_0^{-(m/2)+1}}{A\sigma^p \pi^{p/2} \alpha^p (-(p/2)+1)}$$

$N_f$ – number of cycles required for a crack to grow from $a_0$ to $a_f$. $\alpha$ - is a parameter that depends on the specimen and crack sizes and geometries, as well as the manner of load application.

**Figure-8.14:** *Schematic presentation of fatigue crack growth.*

Increasing mean stress, *R*, in the fatigue cycle has a tendency to increase the crack growth rates in all portions of the curve. The effect of increasing *R* is less in region-II than in regions I and III. The influence of R on the region-II is given by:

$$\frac{da}{dN} = \frac{A(\Delta K)^P}{(1-R)K_c - \Delta K}$$

where $K_c$ – fracture toughness, $R$ – stress ratio. Fatigue life estimation is usually carried out when R=-1 i.e. fully reversed stress conditions, whereas fatigue crack growth data is determined for R=0 i.e. pulsating tension without compression. Compression loads are avoided because during compression loading the crack is closed and the stress intensity factor is zero.

**8.5 Creep, Generalized creep behavior, Stress and Temperature effects**

*8.5.1 Creep*

It is well known and observed number of times that shear modulus of a material increases with decreasing temperature, and this has a corresponding effect on the flow-stress, since the stress associated with a dislocation is always proportional to the shear modulus. Thus $\sigma/E$ can be expected to be constant with varying temperature. However, this ratio
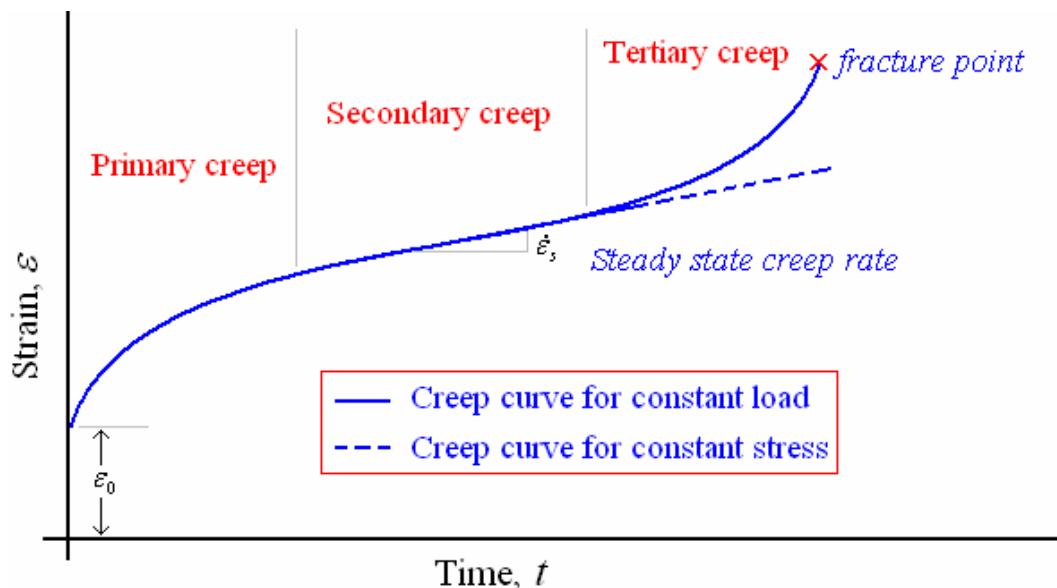
decreases with increase in temperature. Since, the dislocation-density contribution of the flow stress is effectively constant, it was concluded that there must be a second basic component of flow stress that is temperature-dependent i.e.

$$\sigma = \sigma^* + \sigma_E$$

where $\sigma^*$ is thermal component and $\sigma_E$ is athermal component of flow stress. The fact that the flow stress contains a component that responds to thermal activation implies that plastic deformation can occur while both the temperature and the stress are maintained constant. Deformation that occurs under these conditions which is time-dependent is known as *creep*. Creep deformation (constant stress) is possible at all temperatures above absolute zero. However, it is extremely sensitive to temperature. Hence, creep in usually considered important at elevated temperatures (temperatures greater than 0.4 $T_m$, $T_m$ is absolute melting temperature).

### 8.5.2 Generalized creep behavior

Creep behavior of a material is studied using creep test. In creep test, the tensile specimen is subjected to a constant load *or* stress at a constant temperature. Most creep tests are conducted at constant load in analogous to engineering application, whereas creep tests at constant stress are necessary for understanding of mechanism of creep. During the creep test, strain (change in length) is measured as a function of elapsed time. Creep test data is presented as a plot between time and strain known as creep curve. *Figure-8.15* depicts a typical creep curve. The slope of the creep curve is designated as creep rate.



**Figure-8.15:** *Typical creep curve.*

As shown in the above figure, upon loading the specimen, there is an instantaneous deformation ($\varepsilon_0$) that is mostly elastic. Actual creep curve follows this elastic

deformation. Based on the variation of creep rate with time, creep curve is considered to be consists of three portions, each of which has its own distinctive strain-time feature. After initial rapid elongation, $\varepsilon_0$, the creep rate decreases continuously with time, and is known as *primary* or t*ransient creep*. Primary creep is followed by *secondary* or *steady-state* or *viscous creep,* which is characterized by constant creep rate. This stage of creep is often the longest duration of the three modes. Finally, a third stage of creep known as, *tertiary creep* occurs that is characterized by increase in creep rate. Creep curve could be represented by the following equation, according to Andrade:

$$\varepsilon = \varepsilon_0(1 + \beta t^{1/3})e^{kt}$$

where $\varepsilon$ is strain in time $t$, and $\beta$ and $k$ are constants. A better equation is proposed by Garofalo:

$$\varepsilon = \varepsilon_0 + \varepsilon_t(1 - e^{-rt}) + \dot{\varepsilon}_s t$$

where $\varepsilon_0$ – instantaneous strain on loading, $\varepsilon_t$ – limit for transient creep, r – ratio of transient creep rate to the transient creep strain, $\cdot\varepsilon_s$ – steady-state creep rate.

It is suggested that during primary creep, material strain hardens thus increases its creep resistance. Constant creep rate during secondary creep is believed to be due to balance between the competing processes of strain hardening and recovery. The average value of creep rate during the secondary creep is called the minimum creep rate. Third stage creep occurs in constant load tests at high stresses at high temperatures. This stage is greatly delayed in constant stress tests. Tertiary creep is believed to occur because of either reduction in cross-sectional area due to necking or internal void formation. Third stage is often associated with metallurgical changes such as coarsening of precipitate particles, recrystallization, or diffusional changes in the phases that are present.

For metallic materials most creep tests are conducted in uni-axial tensile mode. However, uni-axial compression tests are used for brittle materials to avoid stress amplification and corresponding crack propagation. For most materials creep properties are independent of loading direction.

The minimum creep rate is the most important design parameter derived from the creep curve. It is the engineering design parameter that is considered for long-life applications, e.g. nuclear power plant components. On the other hand, for short-life components (e.g. turbine blades, rocket motor nozzles), time to rupture or rupture lifetime is the dominant factor in design. It is found from test conducted to the point of failure, and the test is known as *stress-rupture test*. This is basically similar to a creep test except that the test is always carried out at higher loads. In a creep test total strain is often less than 0.5%, while in stress-rupture test it is around 50%.

### 8.5.2 Stress and temperature effects

Creep properties of a material are usually characterized at a constant stress and a constant temperature. A change in either of these parameters causes change in creep behavior of the material. With increase in either stress or temperature (a) instantaneous elastic strain increases (b) steady state creep rate increases and (c) rupture lifetime decreases.
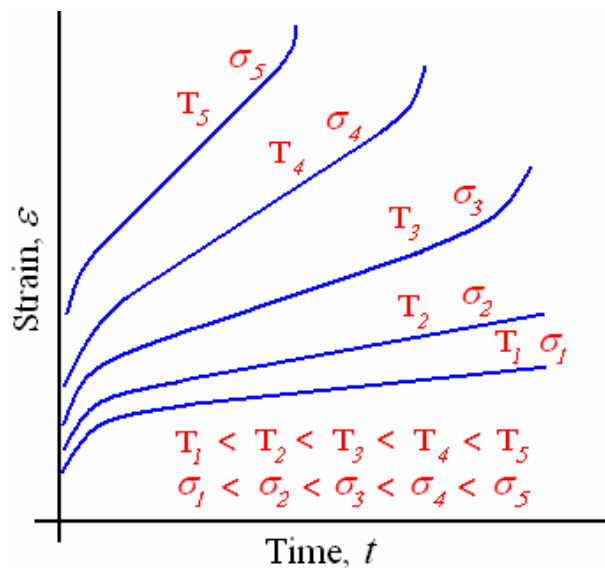
Influence of stress on steady state creep rate can be written as

$$\dot{\varepsilon}_s = K_1 \sigma^n$$

where $K_1$ and $n$ are material constants. Value of these parameters can found from logarithmic plot between creep rate and stress after conducting tests at a constant temperature. Similarly temperature influence on steady state creep rate can be characterized. Influence of combined action of temperature and stress on steady state creep rate can be presented as follows:

$$\dot{\varepsilon}_s = K_2 \sigma^n e^{-\frac{Q_c}{RT}}$$

where $K_2$ and $Q_c$ (activation energy for creep) are constants. Values of n for a specific material are dependent mechanism of creep operational in those particular conditions of stress and temperature. *Figure-8.16* presents the influence of stress/temperature on creep behavior.



**Figure-8.16:** *Influence of stress/temperature on creep behavior.*

Creep data presented in form of stress-temperature diagrams are termed *deformation mechanism maps* which indicates stress-temperature regimes over which various mechanisms operate. The chief creep deformation mechanisms are:

Dislocation glide – involves dislocation moving along slip planes by overcoming barrier with help of thermal activation. This occurs at high stresses, $\sigma/G > 10^{-2}$.

Dislocation creep – involves movement of dislocations which overcome barriers by thermally assisted mechanisms like diffusion of vacancies or interstitials. Occurs at moderate stresses, $10^{-2} > \sigma/G > 10^{-4}$.

Diffusion creep – involves flow of vacancies and interstitials under the influence of applied stress. Occurs for $\sigma/G < 10^{-4}$.

Grain boundary sliding – involves sliding of grains against each other.

It is to be noted that, quite often, more than one creep mechanism will operate at a time. When several mechanisms are in operation at a time simultaneously, i.e. independent of each other, fastest mechanism will dominate the proceedings. On the other hand, when they are operating in series, slowest mechanism will control the creep deformation.

**References**

1. G. E. Dieter, Mechanical Metallurgy, Third Edition, McGraw-Hill, New York, 1986.
2. R. W. Hertzberg, Deformation and Fracture Mechanics of Engineering Materials, Fourth Edition, Wiley, New York, 1996.
3. T. H. Courtney, Mechanical Behavior of Materials, Second Edition, McGraw-Hill, New York, 2000.